GENERAL ATOMICS

PRINCETON PLASMA PHYSICS LABORATORY

β Limits in Intelligent Shell Realizations in DIII-D Geometry*

– M. S. Chu (GA), M. S. Chance and M. Okabayashi (PPPL)

APS Meeting
Quebec City, CANADA
Wednesday, 25 October, 2000

*Work supported by U.S. Department of Energy Grant No. DE-FG03-95ER54309 and DE-FG02-89ER-53297.

Motivation

- Stabilization of the resistive wall mode (RWM) relies on using external coils to replenish the magnetic flux diffused through the resistive shell
- The feedback scheme in DIII-D utilizes a set of active coils, covering only one poloidal segment of the resistive shell on the outboard midplane
- In principle, ideal intelligent shell feedback needs to cover the resistive shell completely with many feedback coils. This may not be practical
- Effective and practical realization of the intelligent shell scheme depends on the size, number and geometry of the coil segments
- The purpose of the present work is to provide a model for evaluating the effectiveness in the realizations of the intelligent shell scheme in toroidal geometry, focusing on poloidal coverage and the number of poloidal segments

Approach

- With the inclusion of a resistive shell and active feedback coils the plasma stability problem in general cannot be treated in the framework of ideal MHD
- However, in a special situation, in which the plasma is surrounded by a resistive shell and a network of '(intelligent) flux conserving coils with $\int \tilde{\psi} ds = 0$' the problem is still treatable by ideal MHD
- This problem has been formulated and computationally implemented by modifying VACUUM and coupled it with GATO
- This allows us perform efficient evaluation of the possible set up of intelligent shells for feedback stabilization
- The effect of feedback on plasma eigenmode structure is included consistently in this approach

MODEL DISPERSION RELATION WITH THE INCLUSION OF DISSIPATION AND A SINGLE PARAMETER τ_W TO CHARACTERIZE THE RESPONSE OF THE RESISTIVE WALL

A uniformly rotating plasma satisfies the cubic dispersion relation

Dissipation

Plasma Potential Energy

$$(\tilde{\gamma} + in\Omega_0)^2 K + (\tilde{\gamma} + in\Omega_0) D + \delta W_p + \frac{\delta W_{vb}\,\tilde{\gamma}\tau_W + \delta W_{v\infty}}{\tilde{\gamma}\tau_W + 1} = 0$$

Kinetic Energy

Perturbed Magnetic Energy in Vacuum

The solution of this dispersion has the following general characteristics:

A stability window in b/b_c opens up when Ω_0 is sufficiently large

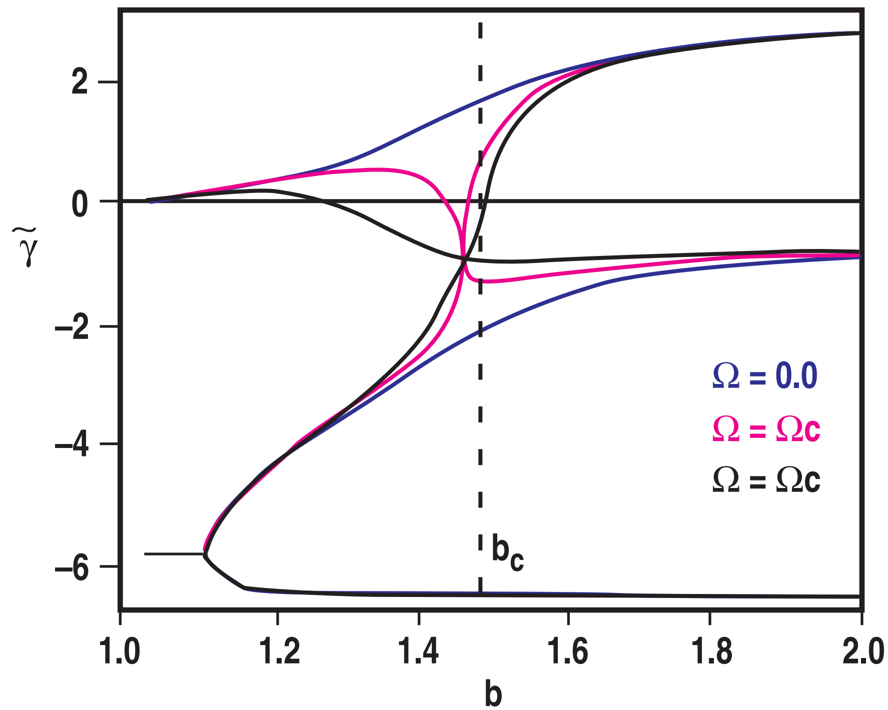

PPPL
PRINCETON PLASMA PHYSICS LABORATORY

GENERAL ATOMICS

201-99 jy

SCHEMATICS OF RWM FEEDBACK ANALYSIS WITH TOROIDAL GEOMETRY

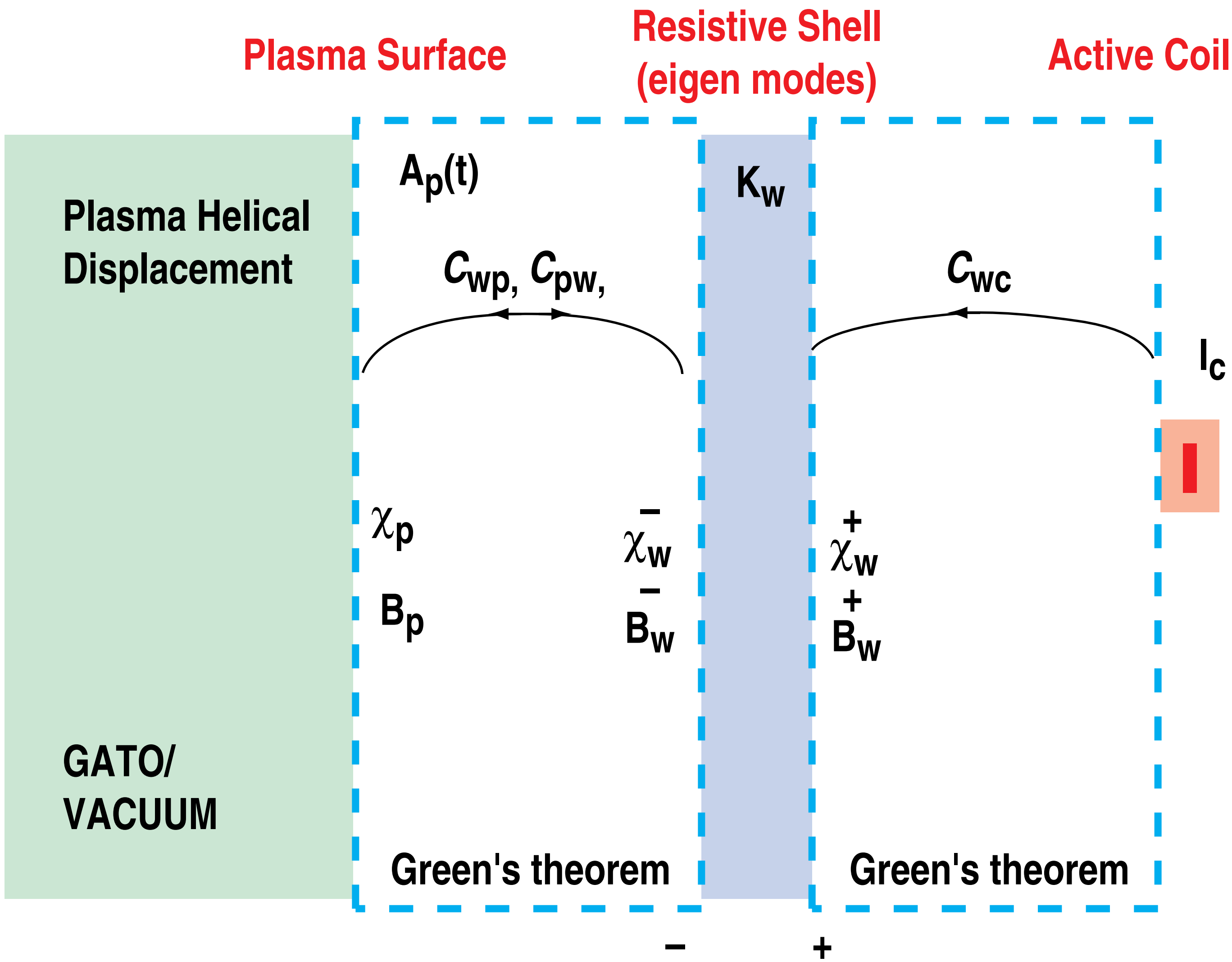

PPPL
PRINCETON PLASMA PHYSICS LABORATORY

GENERAL ATOMICS

MAGNETIC POTENTIAL χ AND GREEN'S FUNCTION SOLUTION

- The magnetic field on the plasma surface and resistive shell are formulated with scalar potential

$$\boldsymbol{B} = \nabla\chi \quad .$$

- With Green's theorem

$$4\pi\overline{\chi}(\vec{r}) + \int_S \chi(\vec{r}\,')\nabla' G(\vec{r},\vec{r}\,') \bullet d\vec{S} = \int_S G(\vec{r},\vec{r}\,')\vec{\nabla}'\overline{\chi}(\vec{r}\,') \bullet d\vec{S}' \quad ,$$

where

$$d\vec{S} = \vec{\nabla} Z\, J\, d\theta d\phi$$

$$2\chi(\vec{\rho}) + (1/2\pi) \int_S e^{in(\phi-\phi')}\chi(\rho')\nabla' G(\vec{r},\vec{r}\,') \bullet d\vec{S} =$$

$$(1/2\pi) \int_S e^{in(\phi-\phi')}\, G(\vec{r},\vec{r}\,')\, \vec{\nabla}'\chi(\vec{\rho}\,') \bullet d\vec{S}' \quad .$$

SOLUTION FOR χ ON THE SURFACES

- The scalar potential, χ, for the magnetic field in the vacuum is solved by the methods of chance, Phys. Plasmas 4 (1997) 2161. It calculated χ as a response to the magnetic perturbations on the surfaces in the vacuum, *i.e.*, the plasma, resistive shell, and feedback coil. We thus have the relations

$$\chi_p\left(\theta_p^i\right) = \sum_{l_p} C_{il_p}(p,p)B_{pl_p} + \sum_{l_w} C_{il_w}^{-}(p,w)B_{wl_w}^{+} \quad .$$

$$\chi_w^{-}\left(\theta_w^i\right) = \sum_{l_p} C_{il_p}^{-}(w,p)B_{pl_p} + \sum_{l_w} C_{il_w}^{-}(w,w)B_{wl_w}^{+} \quad .$$

$$\chi_w^{+}\left(\theta_w^i\right) = \sum_{l_c} C_{il_c}^{+}(w,c)I_c + \sum_{l_w} C_{il_w}^{+}(w,w)B_{wl_w}^{+} \quad .$$

$C_{il_p}^{-}$ (w,p) are Fourier coefficients and $B_{wl_w}^{+}$ coefficients of the shell eigenfunction χ_{lw}

RESIDENTIAL WALL THIN SHELL APPROXIMATION

- Introducing "skin current stream fluction" K_w: $j = \nabla Z \times \nabla K_w \delta (z - z_w)$
- Normal magnetic field continuity $\partial\chi / \partial n (-) = \partial\chi / \partial n (+) = B_n$
- Ampere's law: $\chi(+) - \chi(-) = K_w$
- Faraday's law

$$\nabla_s \bullet [\eta \nabla_s K_w] = \partial/\partial t\,(B_n), \text{ assuming } |\nabla z| = 1$$

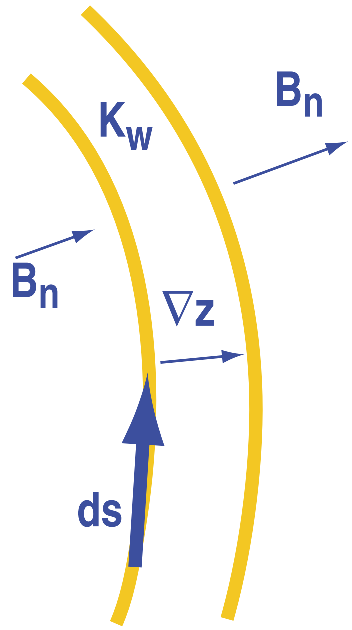

Resistive Shell

$K_w (\theta,\phi)$ can be expanded in eigenmodes

SHELL EIGENFUNCTIONS AND MATCHING CONDITIONS ACROSS THE RESISTIVE SHELL

- The shell eigenfunction χ_{lw} satisfies the equation

$$\overline{\nabla} \bullet \left[\eta \left(\delta \times \delta \chi_{lw} \right) \times \delta_z \right] \equiv \delta_s \bullet \eta \delta_s \chi_{lw} = -\lambda_{lw} \chi_{lw} \quad ,$$

$$\lambda_{lw} > 0 \quad .$$

- We also expand the skin current stream function

$$K_w = \sum_{lw} K_{lw} \chi_{lw} \quad .$$

- Matching across the shell with Maxwell's equations gives

$$\chi^{(+)} - \chi^{(-)} = K_w = -\frac{\mu_0 \Delta Z}{\eta} \sum_{lw} \frac{\partial}{\partial t} \frac{B_{w_{lw}} K_{lw(\theta_w^i)}}{\lambda_{lw}} \quad .$$

FINAL DIAGONALIZATION AND CIRCUIT EQUATIONS

- Defining new variables, $\overline{B}_{w\ell w} = B_{w\ell w} / \lambda_{\ell w}^{1/2}$, ect, and with the transformation matrix $T_{\ell s \ell w}$, we get,diagnolizing the matrix,

$$\left(\frac{\mu_0 \Delta z}{\eta}\frac{\partial}{\partial t} + M_{\ell s}\right)\overline{B}_{\ell s} = -\sum_{\ell_c} \overline{C}_{\ell_s \ell_c}(w,c) I \ell_c + \sum_{\ell_p} \overline{C}_{\ell_s \ell_p}(w,p) B_p \ell_p$$

- The diagonal matrix, $M_{\ell s}$, is given by,

$$M_{\ell_s} \equiv \sum_{\ell_s \ell'w} T^{-1}_{\ell_s \ell'_w} \overline{M}_{\ell'_w \ell_w} T_{\ell_w \ell_s} \quad \textit{with} \quad \overline{M}_{\ell'_w \ell_w} \equiv \lambda^{1/2}_{\ell'_w} M_{\ell'_w \ell_w} \lambda^{1/2}_{\ell'_w}$$

- Here,

$$\overline{B}_{\ell_s} = T^{-1}_{\ell_s \ell_w} \overline{B}_{w,\ell_w}, \quad \overline{C}_{\ell s \ell c}(w,c) = T^{-1}_{\ell_s \ell_w} \overline{C}_{\ell_s \ell_c}(w,c) \ \ \textit{etc.}$$

FULL DISPERSION RELATION WITH INCLUSION OF PLASMA RESPONSE TO FEEDBACK

- For perfect conducting wall, the perturbed vacuum (stabilizing) energy is

$$\delta W_{vb} = \sum_{\ell_p} \sum_{\ell_p'} B_{\ell_p} B_{\ell_p'} C_{\ell_p \ell_p'} \quad .$$

  – With a specific feedback scheme, the feedback coil currents are determined in terms of plasma displacement

  – The leakage magnetic flux through the resistive wall is then also determined by the plasma displacement. The leakage of vacuum (stabilize) energy can then be determined.

PERFECT FEEDBACK THROUGH FLUX LOOPS

- $\Delta \Phi_\ell = 0$ through the loops

$$\delta W_\infty - \delta W_{vb} = \sum_{\ell_p} \sum_{\ell_p'} B_{\ell_p} B_{\ell_p'} G_{\ell_p,\ell_p'} < 0$$

$$G_{\ell_p,\ell_p'} = \sum_{\ell_w} \sum_{\ell_w'} C^{-}_{\ell_p,\ell_w'} C^{-}_{\ell_w',\ell_p'} \lambda^{1/2}_{\ell w} \lambda^{1/2}_{\ell' w} \sum_{\ell_s} \frac{T_{\ell_w,\ell_s} T_{\ell_w',\ell_s}}{\left(\frac{\mu_0 \Delta\delta}{\eta} \gamma + M_{\ell_s}\right)}$$

- The full dispersion relation is

$$(\gamma + in\Omega_0)^2 K + (\tilde{\gamma} + in\Omega_0) D + \delta W_p + \delta W_{vb} + \boxed{(\delta W_\infty - \delta W_{vb})} = 0 \ .$$

Ideal Shell, Intelligent Shell, and its Realizations

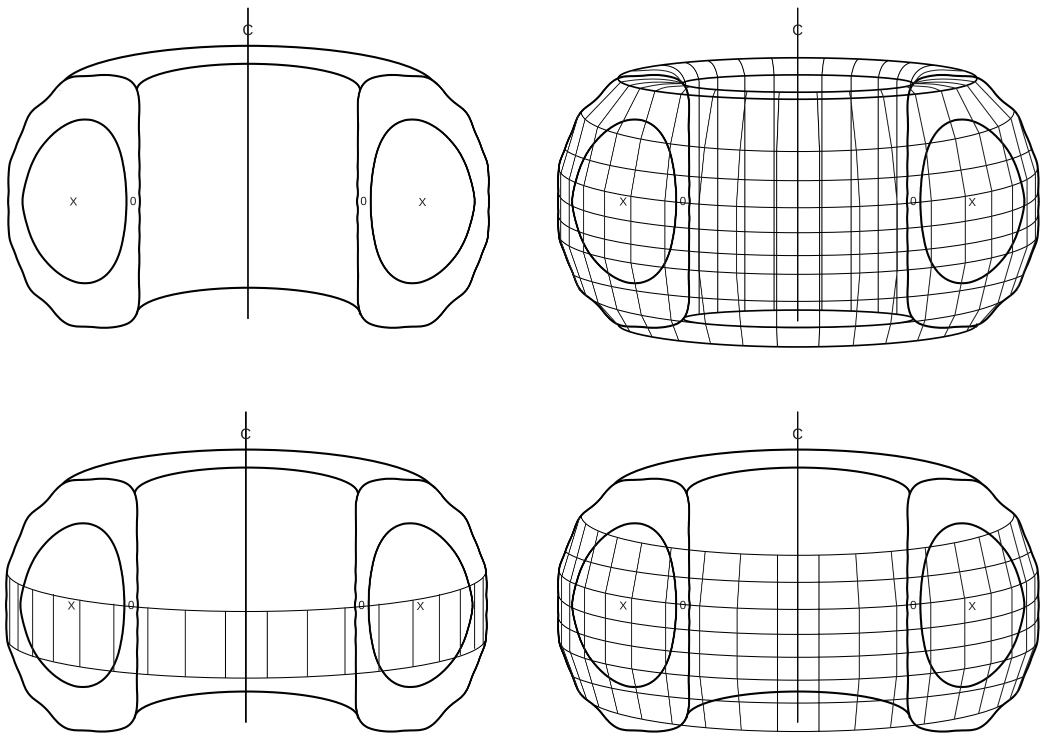

Figure 1: DIII-D shaped plasma in different kinds of shells, top left is for an ideal conducting shell, top right is for an ideal intelligent shell and bottom left is intelligent shell with one poloidal segment and bottom right is intelligent shell with seven poloidal segments

δW is a Measure of the Free Energy

The tokamak plasma is an active medium which can release free enegy to excite MHD instabilities. The vacuum tank is treated as a system of interwoven L/R circuits. When these circuits are excited, flux and energy diffuses through the vacuum tank and plasma stability is reduced

$$\delta W = \delta W_p + \delta W_{VR}$$

$$\delta W_{VR} = \delta W_{V\eta=0} - \delta W_{diff}$$

$$\delta W_{diff} = \sum_{lw} \frac{B_{lw}^2}{(\frac{\mu_0 \Delta\delta}{\eta}\gamma + M_{lw})}$$

The Unstable Mode With an $\eta = \infty$ Shell

shot92544 updown symmetrized, shell total poloidal length=7.63m

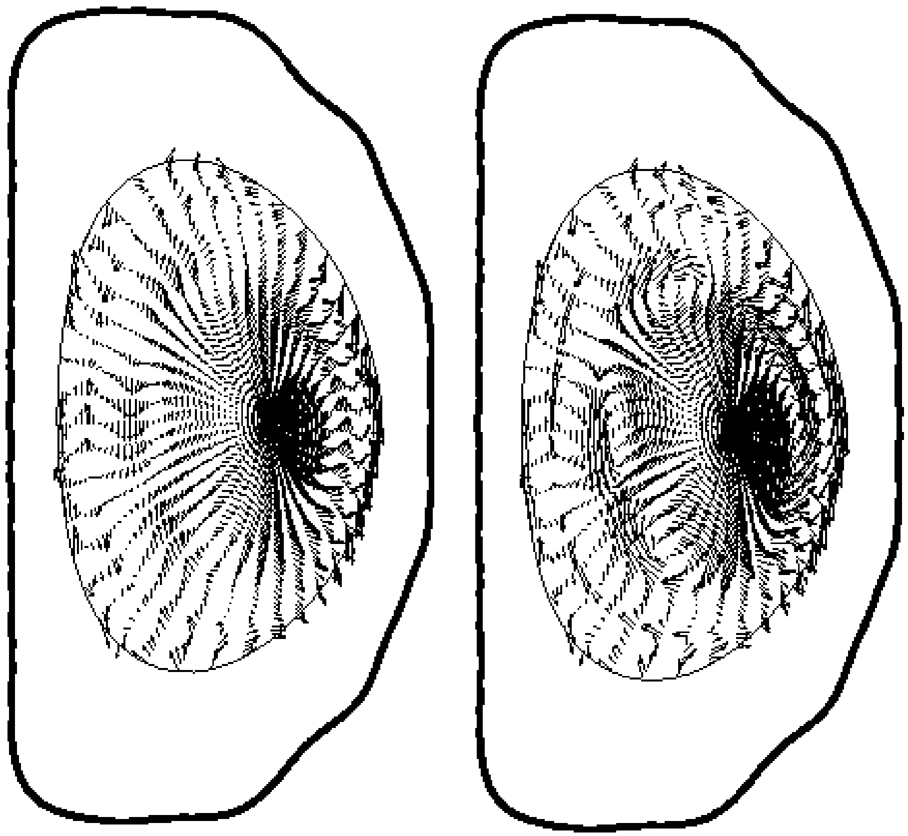

Figure 2: Displacement of plasma surrounded by external shell with large resistivity(left) and 7 segments of flux conserving coils (right)

δW depends on Coverage and Number of Coil Segments

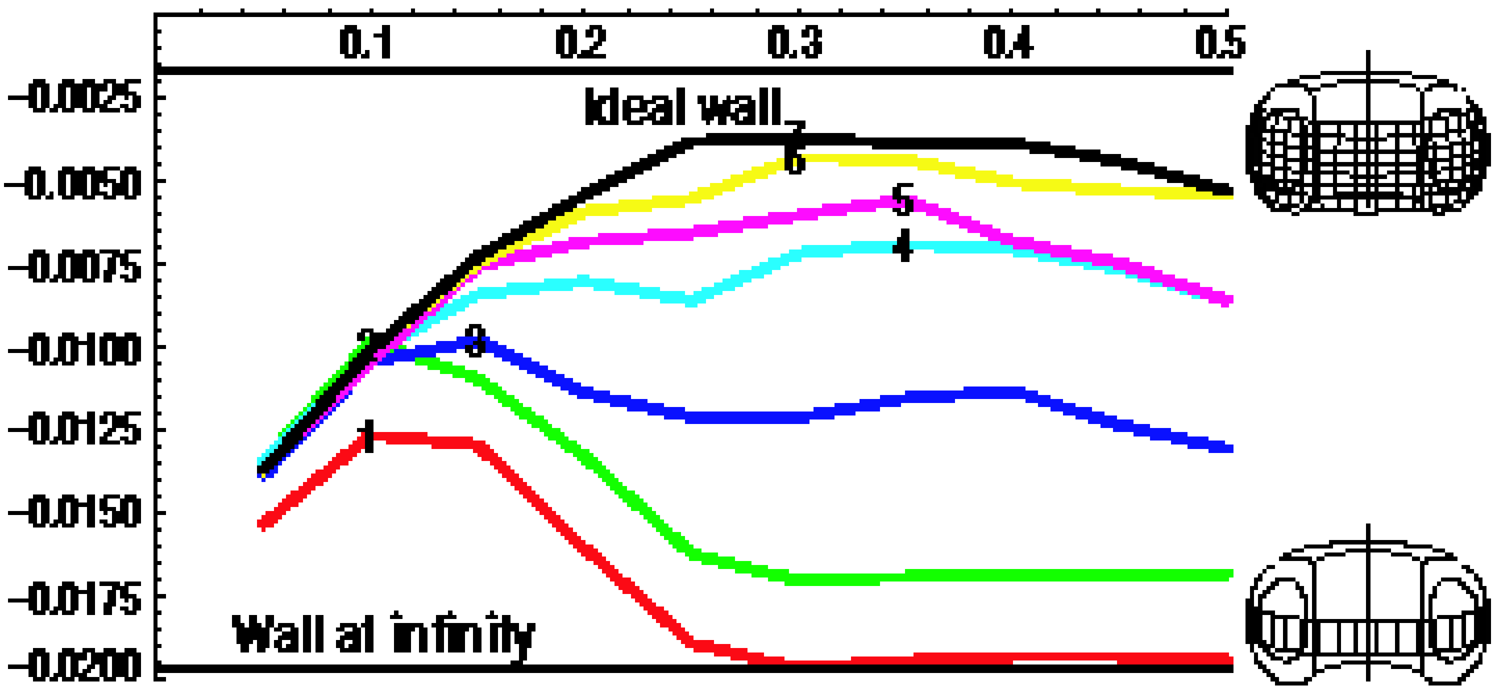

Figure 3: δW vs fractional length of poloidal coverage. The curves are labeled by the number n_s of segments of equal length

Optimum Effectiveness and Coverage vs. Number of Segments n_s

$$E_{ff} = \frac{\delta W_R - \delta W_{\eta=\infty}}{\delta W_{\eta=0} - \delta W_{\eta=\infty}}$$

n_s	Total Coverage	E_{ff}
1	0.129	0.414
2	0.120	0.548
3	0.125	0.564
4	0.346	0.663
5	0.327	0.810
6	0.330	0.863
7	0.280	0.907

Figure 4: dependence of optimum total poloidal length and effectiveness on n_s

Eddy Current Patterns on the Resistive Shell

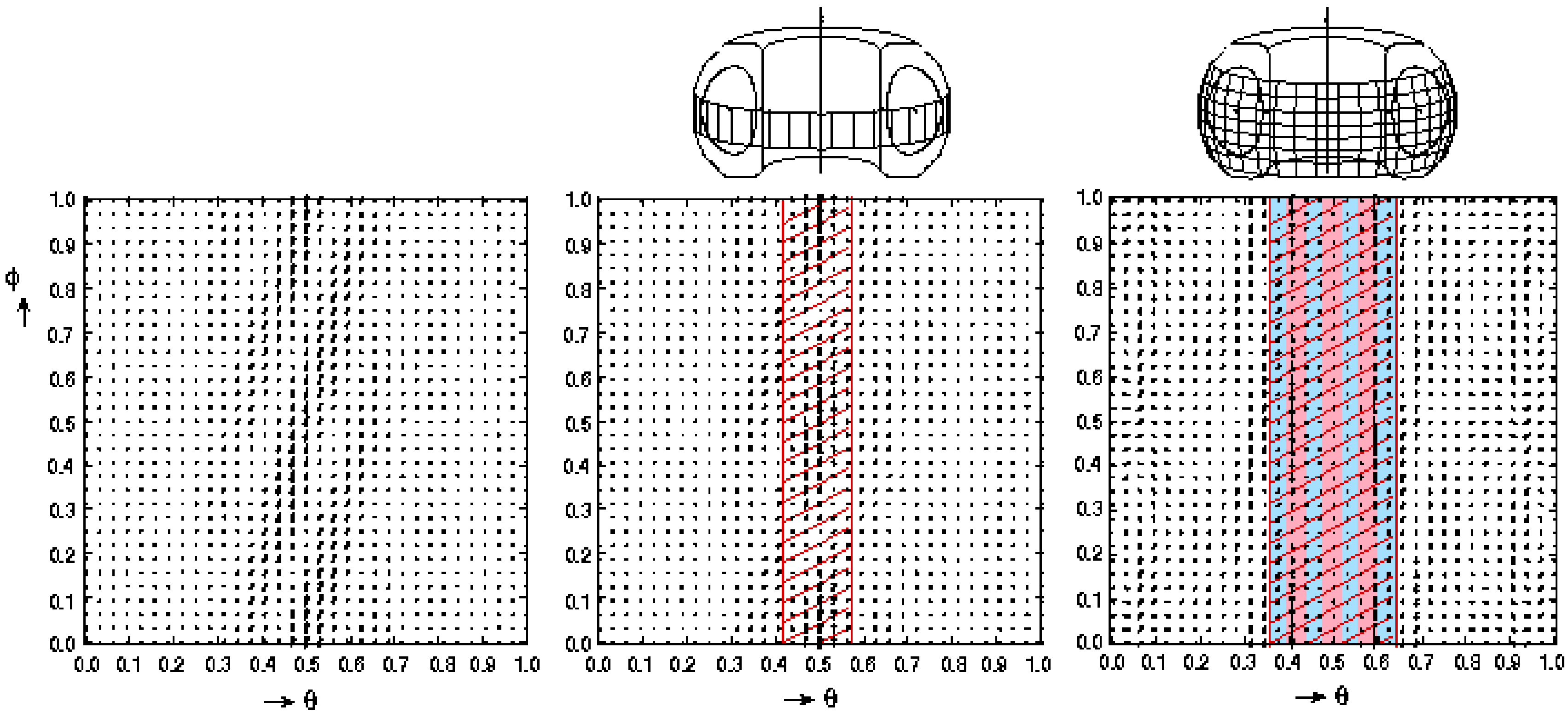

Figure 5: eddy current pattern in the $\theta - \phi$ plane, without feedback (left), optimum of $n_s = 1$ (center) and optimum of $n_s = 7$ (right)

Poloidal and Toroidal Eddy Current Components

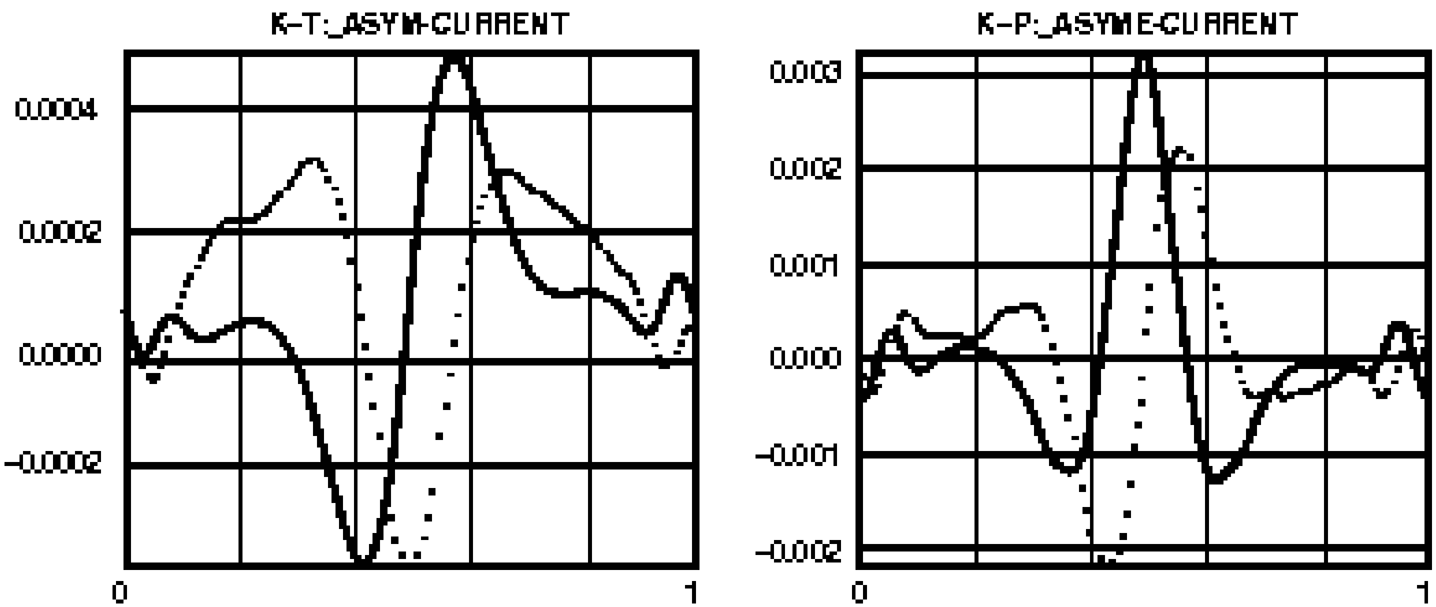

Figure 6: poloidal (b normal) and toroidal amplitudes of eddy currents on the resistive shell with no flux conserving coils, $cos(n\phi)$ component is solid and $sin(n\phi)$ component dotted

Poloidal and Toroidal Eddy Current Components

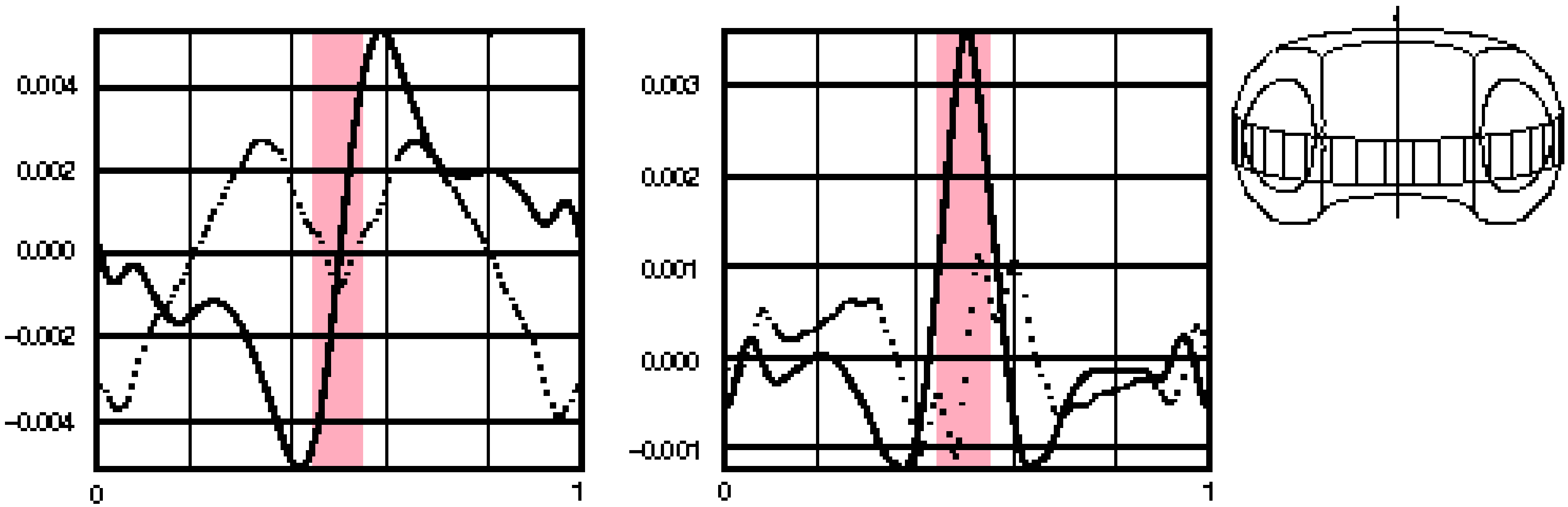

Figure 7: poloidal (b normal) and toroidal amplitudes of eddy currents on the resistive shell with 1 segment of flux conserving coils, $cos(n\phi)$ component is solid and $sin(n\phi)$ component dotted

Poloidal and Toroidal Eddy Current Components

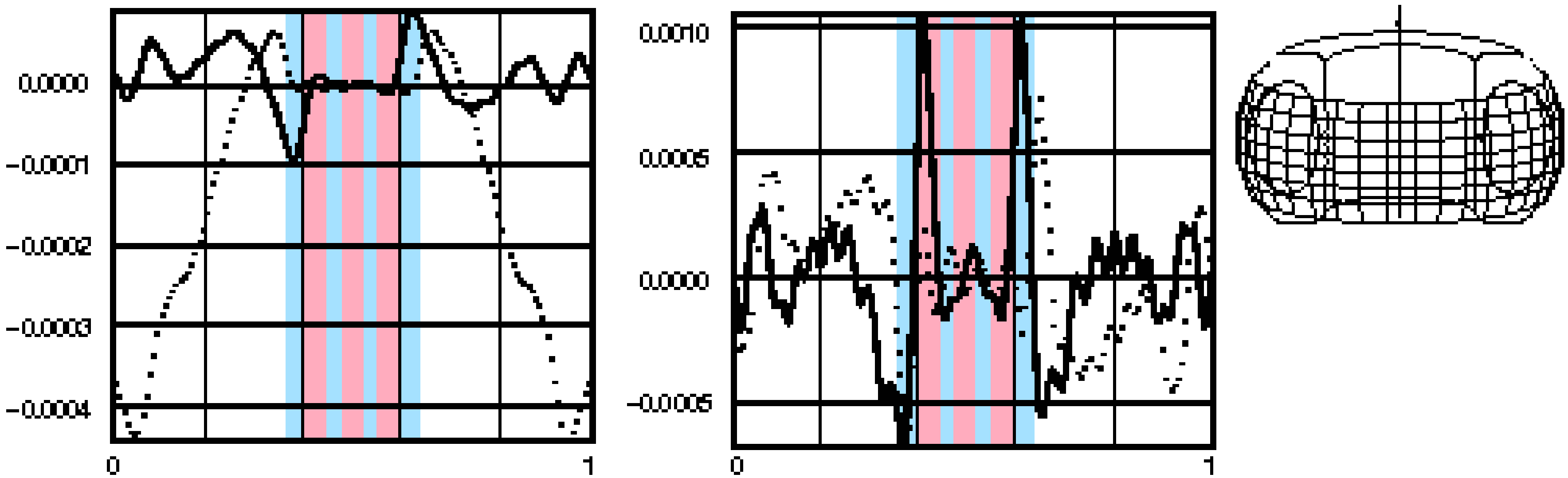

Figure 8: poloidal (b normal) and toroidal amplitudes of eddy currents on the resistive shell with 7 segments of flux conserving coils, $cos(n\phi)$ component is solid and $sin(n\phi)$ component dotted

The Even and Odd Resistive Shell Eigenmodes

The resistive shell eigemodes can be either even or odd with respect to the midplane

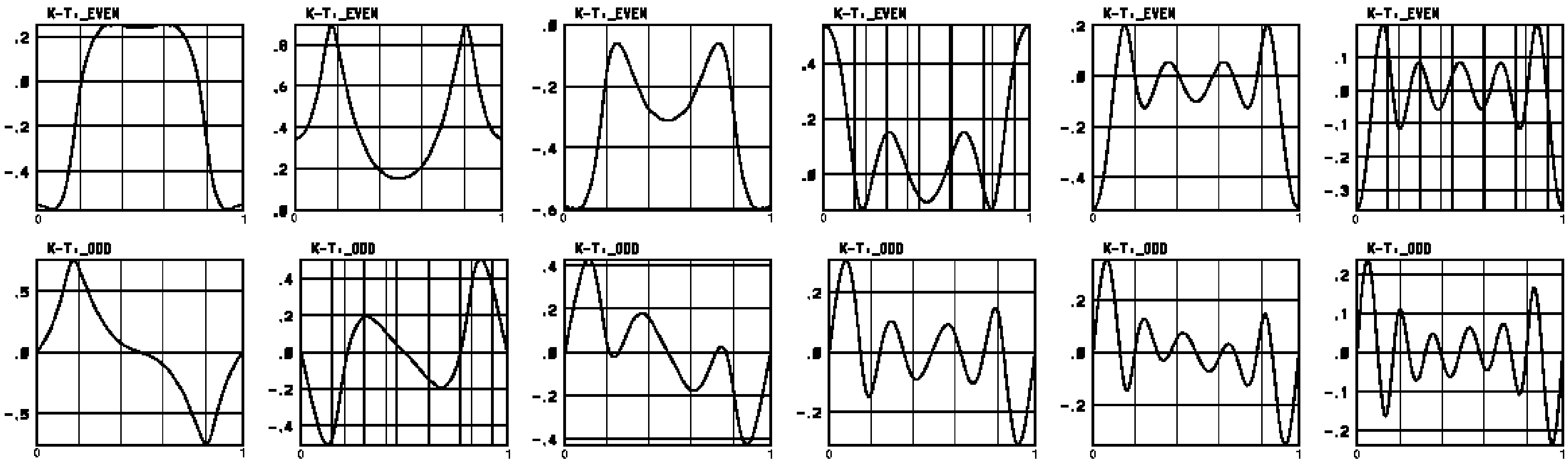

Figure 9: $m = 1$ to $m = 6$ lowest order poloidal even (top) and odd (bottom) eigenfunctions of the resistive shell eigenmodes with the inclusion of the effect of the plasma

Resistive Shell Excitation by Plasma and L/R Shell Times

The resistive shell eigemodes and shell times include effects due to presence of plasma

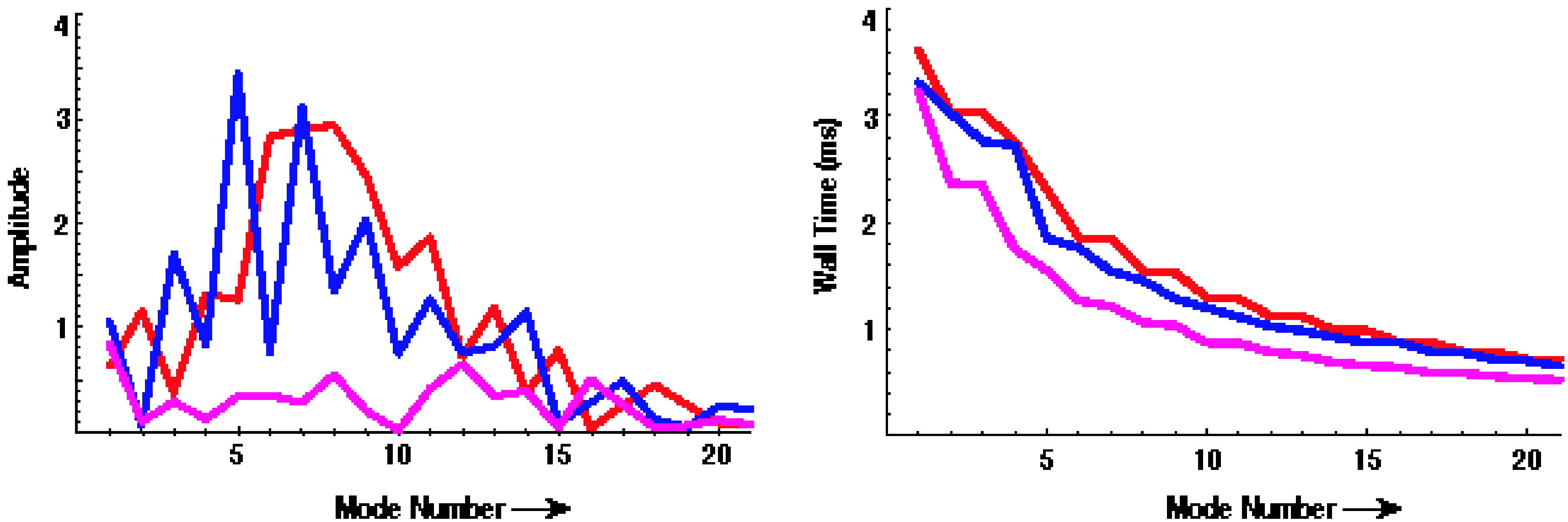

Figure 10: Comparison of excitation amplitudes (left) and shell times (right) of different (resistive shell-plasma) eigenmodes in the three different cases: resistive shell alone, resistive shell with one segment of flux conserving coils , and resistive shell with seven segments of flux conserving coils

Conclusion

- Poloidal coverage of the existing feedback coils is close to being optimum when only one segment of the resistive shell is used for feedback stabilization; with feedback, the shell can be made to be 40% as effective as the ideal shell
- Increasing the number of segments to 6 or 7 and increasing the poloidal coverage to 30% of the total circumference can make the resistive shell up to 90% as effective as an ideal shell
- The GATO code has been coupled to the VACUUM code to perform systematic studies and the time constants and eddy current patterns could be compared with experimental observations
- In the present study and for the chosen equilibrium, mode deformation due to feedback was not significant, rigid helical displacement model could be sufficient